2019-1006 IJOI
http://www.ijoi-online.org/

International Journal of Organizational Innovation

MATHEMATICAL MODELING AND NONLINEAR ANALYSIS OF ADAPTIVE RUBBER BEARINGS

Yien Ji†, C. S. Tsai*, Ying Zhou, H. C. Su, Xilin Lu
†*jiyien19930130@gmail.com*
*cstsai123@gmail.com

Summary

In this study, a new type of seismic isolator, composed of rubber materials and sliding plates called adaptive rubber bearings (ARB's), are proposed. In order to systematically investigate the mechanical behavior of an ARB, mathematical formulations for nonlinear analyses have been derived from the proposed concept of the ARB. Based on the concept of the force equilibrium via the combination of rubber and the sliding core layer by layer, the mathematical formulations presenting the adaptive characteristics of the entire ARB system can be obtained by way of the series of connections of all layers in the entire device. By virtue of the derived mathematical formulations, the phenomena of the ARB isolator possessing adaptive features can be clearly understood even though it is a completely passive device. Numerical analysis which is in good agreement with experimental results infer that the effective stiffness and damping ratio of the ARB isolator change continually during an earthquake and are controllable through appropriate design.

Key Words**:** Seismic isolator, rubber bearing, adaptive rubber bearing

(Editor's Note: This article does not follow the usual two column format of IJOI in order to make the mathematical formulas more readable.)

Introduction

To reduce the seismic response of the existing or new built structures, seismic isolation technology has been known as a promising technique. This has been verified through great amount of experimental and numerical studies. Among the techniques, two types of well-known seismic isolation systems, elastomeric-based system and rolling or sliding-based systems, have been proven to protect the structures from earthquake damage efficiently. In 1870, Jules Touaillon was first granted a patent for base isolation system. This system is located between upper structure and its foundation with two spherical concave and a rolling ball. In1869, the American L. Sterne proposed a patent for railway purposes. Although it was not intended as a means for seismic isolation, it is built up of soft India-rubber rings, and circular or other suitable shaped metal-plates.

This patent is the pioneer of modern seismic isolator. In 1978, William H. Robinson of New Zealand proposed a base isolator called the Lead Rubber Bearing (LRB) by inserting a lead plug into a laminated rubber bearing which was proposed by L. Sterne in 1869. Among these technologies, the lead rubber bearing has been most popular. However, the LRB that uses a lead material has resulted in environment problems and been prohibited by many well developed countries. In addition, many researchers have urged that the temperature of the LRB will rise after absorbing seismic energy to weaken materials and functions of the isolators. This causes larger displacements than we would expect. Both LRB and HDRB possess a feature of too small damping for engineering practice and need supplemental damping from other dampers, which will cause increased expenses and longer construction time as well as need more spaces to install additional dampers.

In order to solve abovementioned problems, this study proposes a new rubber bearing called Adaptive Rubber Bearing (ARB). These isolators are the combination of rubber and the sliding core layer. The proposed rubber bearings are completely passive, yet possess adaptive characteristics of stiffness and damping. Compared with the traditional lead rubber bearings, the ARB has the following advantages: (1)using environmentally friendly materials; (2) having no problem of internal temperature rise; (3) Uniform stress distribution of the energy dissipation unit no stress concentration problem at the center of the support pad; (4) has a high damping ratio; (5) has self-adapting characteristics; (6) is easy to manufacture; (7) is light in weight; and (8) Under different levels of earthquakes, different rubber layers are deformed to achieve self-adaptation optimization; and (9) The vertical stiffness can be adjusted through the combination of different sliding materials, not only related to the rubber layer. In this study, experimental results are provided to verify the concept of the proposed device. The ARB has a damping ratio close to 60% at small displacements. Such high damping characteristics not only need no additional damping devices in the engineering application for enhancing the damping ratio, but also are simpler in design. In addition, the damping ratio of the ARB isolator change continually during an earthquake and controllable through appropriate design.

Concept Of Proposed Adaptive Rubber Bearings

Model overview

In this section, the major concept of ARB will be described as follow.
As shown in Figure 1, the adaptive rubber bearing consist of alternate rubber layers and shim plates that similar to the traditional rubber bearings. However, the major different of the proposed isolators is a new sliding core, which is composed of sliding plates located at each layer of rubber to form the sliding surface that are confined by two adjacent shim plates. The friction coefficient of the sliding surface can be different from one sliding interface or rubber layer to another, which can control the timing of initiating the sliding motion of a sliding plate or rubber layer. There will be two situations as follow:

1. When the total horizontal force of a layer is less than the static friction force of the layer, the layer will not deform or slip horizontally, so the layer does not contribute any damping ratio to the isolator as a whole. In addition, the horizontal stiffness of this layer is considered to be infinite.

2. When the total horizontal force of a layer exceeds the static friction force of the layer, the layer will produce relative movement accompanied by rubber shear deformation, which can not only provide some damping, but also contribute flexibility to the isolation system. In addition, the relative sliding of two adjacent sliding interfaces will occur, which can provide a certain degree of friction damping. At this time, the mechanical behavior of the overall isolator should be a series of sliding layers located at different layers where movements exist. By adjusting the friction coefficients of different sliding interfaces, the effect of adaptive characteristics and high damping ratio can be achieved.

From the above, we can see that the isolator can adjust itself by adjusting the friction coefficient of each layer, the size of sliding surface and the thickness and material of rubber, and then combine the above parameters to adjust the isolator's different behavior under different magnitude earthquakes.

Theoretical Effective Stiffness, Damping Ratio and Mathematical Model

Nonlinear Mathematical Model for ARB Devices.

In this section, a nonlinear mathematical model is derived to simulate the mechanical behavior of the proposed seismic isolator.

Figure 2 shows that the total horizontal force of the i^{th} layer in the device is the sum of the shear force of the rubber material and the frictional force of the sliding plate.

This is given as:

$$F_i = f_{ri} + f_{fi} \tag{1}$$

Based on the Wen's model, the following equation to simulate the mechanical behavior of the rubber material.

$$\begin{aligned} f_{ri} &= \alpha_i \frac{F_i^y}{Y_i} u_i + (1-\alpha_i) F_i^y Z_i(t) + c_i v_i \\ &= \alpha_i \frac{F_i^y}{Y_i} du_i + (1-\alpha_i) F_i^y dZ_i(t) + F_{ri}^p + c_i v_i \end{aligned} \tag{2}$$

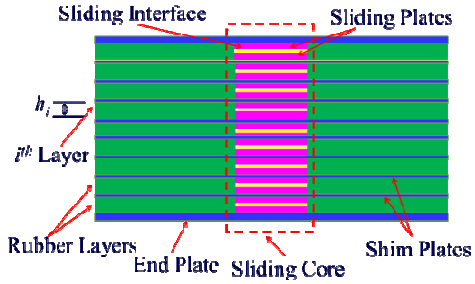

Figure 1. Sketch of adaptive rubber bearing

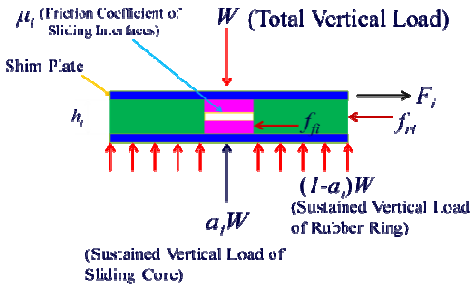

Figure 2. Total force in a layer of ARB

where F_i^y and Y_i represent the yield force and yield displacement, respectively; α_i denotes the ratio of the post-yielding to pre-yielding stiffness; c_i is the damping coefficient for defining the velocity dependent damping force of the rubber material; F_{ri}^P defines the plastic force of rubber material at the previous time which is velocity independent and Z_i and dZ_i denotes a dimensionless variable and increment that control the plastic behavior of the rubber material in the i^{th} layer and is given by:

$$\frac{dZ_i}{dt}Y_i = A_i\frac{du_i}{dt} - Z_i^2\left[\gamma_i \mathrm{sgn}\left(\frac{du_i}{dt}Z_i\right) + \beta_i\right]\frac{du_i}{dt} \tag{3}$$

which results in

$$dZ_i = \frac{A_i}{Y_i}du_i - \frac{Z_i^2 Q_i(t)}{Y_i}du_i = \left(\frac{A_i}{Y_i} - \frac{Z_i^2 Q_i(t)}{Y_i}\right)du_i \tag{4}$$

where:

$$\mathrm{Q}_i(t) = \gamma \mathrm{sgn}\left(dU_i(t)\cdot Z_i(t)\right) + \beta \tag{5}$$

A_i, γ_i, and β_i are dimensionless quantities that control the shape of the hysteresis loop. Note that many other mathematical models can be used to simulate the nonlinear behavior of the rubber material.

If we set $Z_i = Z_p + dZ_i$, then Eq. (4) can be rewritten as:

$$dZ_i^2(t) + \left(\frac{Y}{Q_i(t)du_i(t)} + 2Z_{pi}(t)\right)dZ_i(t) + \left(Z_{pi}^2(t) - \frac{A}{Q_i(t)}\right) = 0 \tag{6}$$

where Z_{Pi} is the dimensionless variable at the previous time.

The solution to Eq. (6) is given by:

$$dZ_i(t)=\frac{1}{2}\left\{-\left[\frac{Y}{Q_i(t)du_i(t)}+2Z_{pi}(t)\right]\pm\sqrt{\left[\frac{Y}{Q_i(t)du_i(t)}+2Z_{pi}(t)\right]^2-4\left[Z_{pi}^2(t)-\frac{A}{Q_i(t)}\right]}\right\} \quad (7)$$

The frictional force of the sliding interface of the sliding plates in the i^{th} layer can be modeled by the following.

$$f_{fi}=a_iW\mu_i\,\mathrm{sgn}(v_i) \quad (8)$$

where $\mathrm{sgn}(v_i)$ is the sign of the sliding velocity of the i^{th} layer.

Note that the total horizontal force of the device in the i^{th} layer is the sum of the shear force of rubber and the frictional force of the sliding plate.

The following equation can be obtained by substituting Eqs. (2), (4) and (8) into Eq. (1):

$$\begin{aligned}F_i&=f_{ri}+f_{fi}=\alpha_i\frac{F_i^y}{Y_i}du_i+(1-\alpha_i)F_i^y dZ_i(t)+F_{ri}^P+c_iv_i+a_iW\mu_i\,\mathrm{sgn}(v_i)\\&=\frac{F_i^y}{Y_i}\left[\alpha_i+(1-\alpha_i)\left(A_i-Z_i^2Q_i(t)\right)\right]du_i(t)+F_{ri}^P+c_iv_i+a_iW\mu_i\,\mathrm{sgn}(v_i)\\&=k_i(t)du_i(t)+F_{ri}^P+c_iv_i+a_iW\mu_i\,\mathrm{sgn}(v_i)\end{aligned} \quad (9)$$

where $k_i=\frac{F_i^y}{Y_i}\left[\alpha_i+(1-\alpha_i)\left(A_i-Z_i^2Q_i(t)\right)\right]$

Rearranging Eq. (9) yields:

$$F_i-F_{ri}^{\mathrm{P}}-c_iv_i-a_iW\mu_i\,\mathrm{sgn}(v_i)=k_idu_i \quad (10)$$

From Eq. (10), the displacement increment of the i^{th} layer can be obtained by:

$$du_i=\frac{1}{k_i}\left[F_i-F_{ri}^P-c_iv_i-a_iW\mu_i\,\mathrm{sgn}(v_i)\right] \quad (11)$$

If the horizontal force sustained by the sliding plates is smaller than the frictional force in the n^{th} layer, $a_nW\mu_n$, the total displacement increment of the device is the sum of all layers except for the n^{th} layer in the isolator. This yields:

$$du = \sum_{\substack{i=1 \\ i\neq n}}^{N} du_i = \sum_{\substack{i=1 \\ i\neq n}}^{N} \frac{1}{k_i}\left[F_i - F_{ri}^{P} - c_i v_i - a_i W \mu_i \operatorname{sgn}(v_i)\right] \tag{12}$$

Rearranging Eq. (12), we obtain:

$$du + \sum_{\substack{i=1 \\ i\neq n}}^{N} \frac{1}{k_i}\left[F_{ri}^{P} + c_i v_i + a_i W \mu_i \operatorname{sgn}(v_i)\right] = \sum_{\substack{i=1 \\ i\neq n}}^{N} \frac{F_i}{k_i} = F \sum_{\substack{i=1 \\ i\neq n}}^{N} \frac{1}{k_i} \tag{13}$$

Rearranging Eq. (13) yields:

$$\begin{aligned} F &= \frac{1}{\sum_{\substack{i=1 \\ i\neq n}}^{N} \frac{1}{k_i}} \left\{ du + \sum_{\substack{i=1 \\ i\neq n}}^{N} \frac{1}{k_i}\left[F_{ri}^{P} + c_i v_i + a_i W \mu_i \operatorname{sgn}(v_i)\right] \right\} \\ &= K_{\tan} du + K_{\tan} \sum_{\substack{i=1 \\ i\neq n}}^{N} \frac{1}{k_i}\left[F_{ri}^{P} + c_i v_i + a_i W \mu_i \operatorname{sgn}(v_i)\right] \\ &= K_{\tan} du + F_D \end{aligned} \tag{14}$$

Therefore, if the n^{th} layer is not activated, the tangential stiffness of the whole device in the horizontal direction can be obtained as:

$$K_{\tan} = \frac{k_2 k_3 .... k_{n-1} k_{n+1} .... k_N + ... + k_1 k_2 k_3 .. k_{n-1} k_{n+1} .. k_{N-1}}{k_1 k_2 k_3 ... k_{n-1} k_{n+1} ..... k_{N-1} k_N} \tag{15}$$

The damping force of the entire system, F_D, can be expressed as:

$$F_D = K_{\tan} \sum_{\substack{i=1 \\ i\neq n}}^{N} \frac{1}{k_i}\left[F_{ri}^{P} + c_i v_i + a_i W \mu_i \operatorname{sgn}(v_i)\right] \tag{16}$$

For a special case in which the same material properties are used in all layers, the tangential stiffness of the whole device in the horizontal direction can be obtained as:

$$K_{\tan} = \frac{k_i}{N} \tag{17}$$

and the damping force is given by:

$$\begin{aligned} F_D &= F_{ri}^P + c_i v_i + a_i W \mu_i \operatorname{sgn}(v_i) \\ &= F_{ri}^P + \frac{c_i}{N} v + aW\mu \operatorname{sgn}(v_i) \end{aligned} \tag{18}$$

Where v is the total horizontal velocity of the device.

Theoretical Effective Stiffness and Equivalent Damping Ratio for ARB Devices.

In this section, theoretical effective stiffness and equivalent damping ratio will be determined (Tsai et al. 2018).

Referring to Figure 3 and 4, the enclosed area of the hysteretic loop of the rubber material is obtained as:

$$A_{ri} = 2\pi k_{eff}^{ri} u_i^2 \xi_{ri} \tag{19}$$

The enclosed area of the hysteretic loop of the sliding plate is given by:

$$A_{fi} = 4u_i f_{fi} = 4(\mu_i a_i W)u_i \tag{20}$$

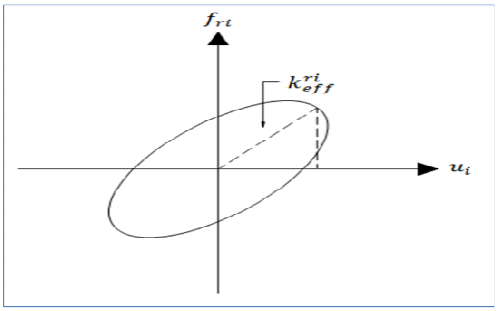

Figure 3. Hysteresis loop of a single layer of rubber material

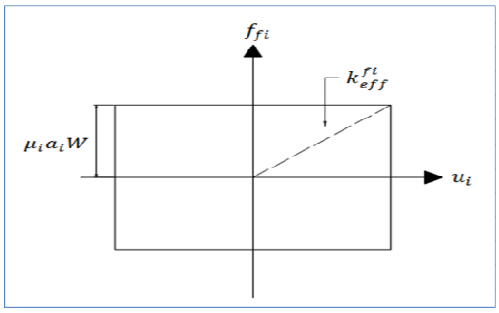

Figure 4. Hysteresis loop of a sliding core in a single layer

The effective stiffness of the sliding plates is

$$k_{eff}^{fi} = \frac{f_{fi}}{u_i} = \frac{\mu_i a_i W}{u_i} \tag{21}$$

The effective stiffness of a typical layer is

$$k_{eff}^{i} = k_{eff}^{ri} + \frac{\mu_i a_i W}{u_i} \tag{22}$$

The horizontal force in a single layer is

$$F_i = (k_{eff}^{ri} + k_{eff}^{fi}) u_i = k_{eff}^{ri} u_i + a_i W \mu_i \tag{23}$$

Arranging the above equation yields

$$u_i = \frac{F_i - a_i W \mu_i}{k_{eff}^{ri}} \tag{24}$$

The total displacement of the isolator is

$$u = \sum_{\substack{i=1 \\ i \neq n}}^{N} u_i = \sum_{\substack{i=1 \\ i \neq n}}^{N} \frac{F_i - a_i W \mu_i}{k_{eff}^{ri}} = F \sum_{\substack{i=1 \\ i \neq n}}^{N} \frac{1}{k_{eff}^{ri}} - \sum_{\substack{i=1 \\ i \neq n}}^{N} \frac{a_i W \mu_i}{k_{eff}^{ri}} \tag{25}$$

Arranging the above equation leads to

$$F = \frac{1}{\sum_{\substack{i=1 \\ i \neq n}}^{N} \frac{1}{k_{eff}^{ri}}} u + \frac{1}{\sum_{\substack{i=1 \\ i \neq n}}^{N} \frac{1}{k_{eff}^{ri}}} \sum_{\substack{i=1 \\ i \neq n}}^{N} \frac{a_i W \mu_i}{k_{eff}^{ri}} \tag{26}$$

The effective stiffness of sole rubber layers is given by:

$$\begin{aligned} \frac{1}{K_{eff}^{rb}} &= \sum_{\substack{i=1 \\ i \neq n}}^{N} \frac{1}{k_{eff}^{ri}} = \frac{1}{k_{eff}^{r1}} + \frac{1}{k_{eff}^{r2}} + \frac{1}{k_{eff}^{r3}} + ... + \frac{1}{k_{eff}^{rn-1}} + \frac{1}{k_{eff}^{rn+1}} .. + \frac{1}{k_{eff}^{rN}} \\ &= \frac{k_{eff}^{r2} k_{eff}^{r3} .... k_{eff}^{rn-1} k_{eff}^{rn+1} .... k_{eff}^{rN} + ... + k_{eff}^{r1} k_{eff}^{r2} k_{eff}^{r3} .. k_{eff}^{rn-1} k_{eff}^{rn+1} ..... k_{eff}^{rN-1}}{k_{eff}^{r1} k_{eff}^{r2} k_{eff}^{r3} ... k_{eff}^{rn-1} k_{eff}^{rn+1} ..... k_{eff}^{rN-1} k_{eff}^{rN}} \end{aligned} \tag{27}$$

The governing equation in terms of effective stiffness for the entire bearing is given by:

$$F = K_{eff}^{rb} u + K_{eff}^{rb} \sum_{\substack{i=1 \\ i \neq n}}^{N} \frac{a_i W \mu_i}{k_{eff}^{ri}} = K_{eff}^{rb} u + F_{eff}^{f} \tag{28}$$

The displacement of a single layer by substituting Eq. (28) into Eq. (24) can be obtained as:

$$u_i = \frac{F_i - a_i W \mu_i}{k_{eff}^{ri}} = \frac{F - a_i W \mu_i}{k_{eff}^{ri}} = \frac{1}{k_{eff}^{ri}} \left[\left(K_{eff}^{rb} u + K_{eff}^{rb} \sum_{\substack{i=1 \\ i \neq n}}^{N} \frac{a_i W \mu_i}{k_{eff}^{ri}} \right) - a_i W \mu_i \right] \tag{29}$$

Substitution of Eq. (29) into Eq. (19) leads to the enclosed area of the hysteretic loop of rubber in a single layer

$$A_{ri} = \frac{2\pi\xi_{ri}}{k_{eff}^{ri}} \left[\left(K_{eff}^{rb} u + K_{eff}^{rb} \sum_{\substack{i=1 \\ i \neq n}}^{N} \frac{a_i W \mu_i}{k_{eff}^{ri}} \right) - a_i W \mu_i \right]^2 \tag{30}$$

Substitution of Eq. (29) into Eq. (20) results in the enclosed area of the hysteretic loop of the sliding plate in a single layer

$$A_{fi} = 4(\mu_i a_i W) u_i = \frac{4\mu_i a_i W}{k_{eff}^{ri}} \left[\left(K_{eff}^{rb} u + K_{eff}^{rb} \sum_{\substack{i=1 \\ i \neq n}}^{N} \frac{a_i W \mu_i}{k_{eff}^{ri}} \right) - a_i W \mu_i \right] \tag{31}$$

Combination of Eqs. (30) and (31) yields the equivalent damping ratio of the entire isolator

$$\begin{aligned} \xi_e &= \frac{1}{2\pi K_{eff} u^2} \sum_{\substack{i=1 \\ i \neq n}}^{N} \left(A_{ri} + A_{fi} \right) \\ &= \frac{1}{2\pi K_{eff} u^2} \left\{ \sum_{\substack{i=1 \\ i \neq n}}^{N} \frac{2\pi\xi_{ri}}{k_{eff}^{ri}} \left[\left(K_{eff}^{rb} u + K_{eff}^{rb} \sum_{\substack{i=1 \\ i \neq n}}^{N} \frac{a_i W \mu_i}{k_{eff}^{ri}} \right) - a_i W \mu_i \right]^2 \right\} \\ &+ \frac{1}{2\pi K_{eff} u^2} \left\{ \sum_{\substack{i=1 \\ i \neq n}}^{N} \frac{4\mu_i a_i W}{k_{eff}^{ri}} \left[\left(K_{eff}^{rb} u + K_{eff}^{rb} \sum_{\substack{i=1 \\ i \neq n}}^{N} \frac{a_i W \mu_i}{k_{eff}^{ri}} \right) - a_i W \mu_i \right] \right\} \end{aligned} \tag{32}$$

As a special case, when the same material properties are used in all layers, then the effective stiffness of the entire isolator with uniform properties can be expressed as:

$$K_{eff} = K_{eff}^{rb} + \frac{aW\mu}{u} \tag{33}$$

The equivalent damping ratio of the whole rubber bearing is given by:

$$\xi_e = \frac{\xi_e^{rb}}{1+\frac{aW\mu}{K_{eff}^{rb}u}} + \frac{2}{\pi}\frac{1}{1+\frac{K_{eff}^{rb}u}{aW\mu}} \tag{34}$$

Comparison Of Experimental And Analytical Results

In this section, test results of a full-scale ARB are presented to validate the mechanical behavior of ARB in this study. Figure 5 shows the detail of full-scale ARB. The full-scale ARB is 700mm in diameter, and a 5 mm cover, 16 layers of rubber, a sliding core in 300mm, and 15 shim plates in 4mm. Each layers of rubber are 4mm thick and three sliding plates with the same thickness as rubber.

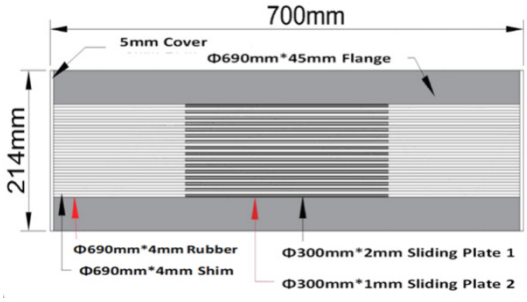

Figure 5. Detail of full-scale ARB Specimen

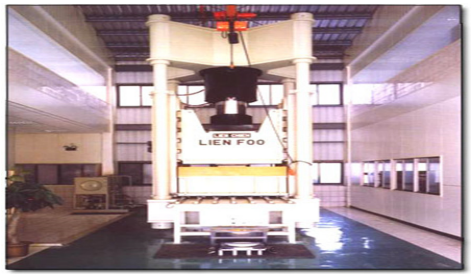

Figure 6. Photo of testing machine

These sliding plates are located between two shim plates to form two major sliding interfaces. The choice of the material of sliding plates depend on their vertical stiffness, friction coefficient, strength, wear resistance, specific heat and melting temperature. Figure 6 shows the test set-up for the ARB located at Tauyan Laboratory of CECI Nova Technology Co., Ltd., Taiwan. The capacity of Biaxial Loading Test Machine is 9810kN in vertical direction, 981kN and a displacement 225mm in horizontal direction.

Figure 7-10 show the hysteresis loops while the full-scale specimen is subjected to 100%, 150%, 200% and 250% of shear strain in rubber, and under a vertical load 3740kN, known as vertical pressure 10MPa.

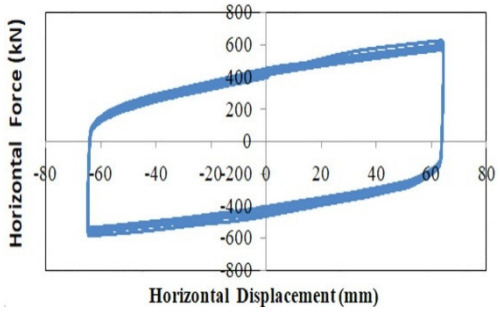

Figure 7. Hysteresis loops at strain of 100% strain of 150% under pressure of 10MPa.

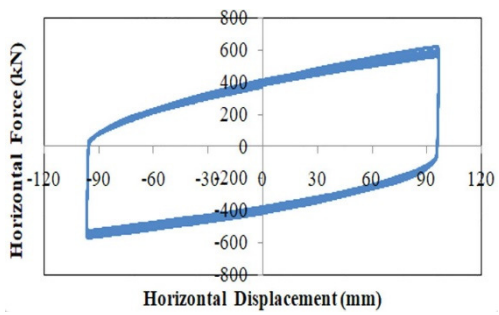

Figure 8. Hysteresis loops at under pressure of 10MPa.

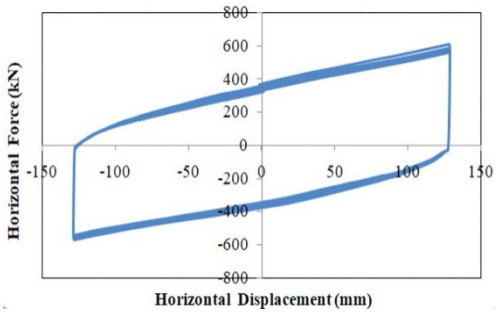

Figure 9. Hysteresis loops at strain of 200% strain of 250% under pressure of 10MPa.

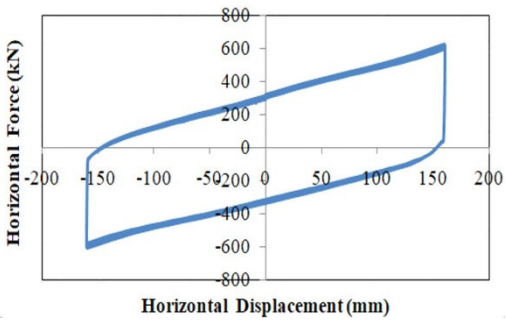

Figure 10. Hysteresis loops at under pressure of 10MPa.

Figures 11 and 12 respectively present the comparison of the analytical and experimental results of the effective stiffness and equivalent damping ratio of the ARB. The damping ratio is 55.99% at the shear strain of 50%, 49.37% at the shear strain of 100%and 35.09% at the shear strain of 250%, which compare with the analytical results.

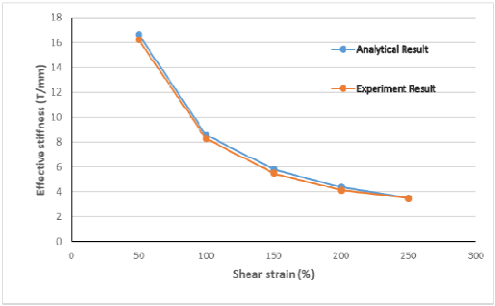

Figure 11. Effective stiffness at various levels levels of strains under pressure of 10MPa.

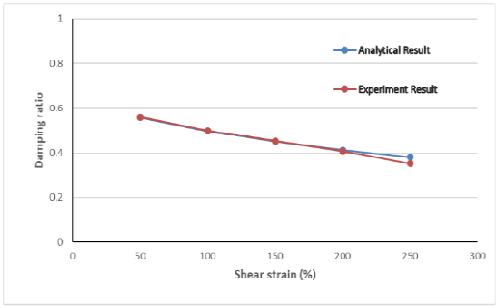

Figure 12. Damping ratio at various of strain under pressure of 10MPa.

In addition, Figures 13 and 14 show the analytical results of hysteresis loops. The test results as shown in Figures 7 and 9 prove that the ARB isolator provides high damping ratio to absorb seismic energy and that a good agreement between the analytical and experimental results has been obtained.

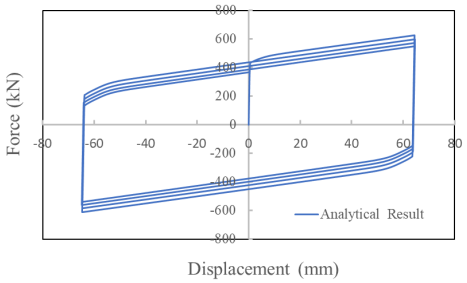

Figure 13. Analytical result at the strain of strain of 100% under pressure of 10MPa

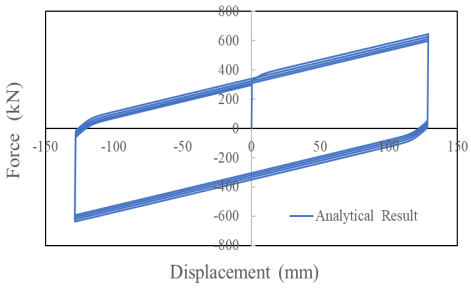

Figure 14. Analytical result at the 200% under pressure of 10MPa

Conclusions

Innovative rubber bearings called adaptive rubber bearings were proposed in this study. The following conclusions can be drawn:

1. The ARB isolators use lead- free materials that are environmentally friendly.

2. The proposed rubber bearings are completely passive devices but possess adaptive characteristics.

3. The decrease in equivalent damping ratio of the ARB with an increased displacement is not considerable.
4. The ARB isolator has much higher damping ratio than the LRB and HDRB.

5. The mechanical behavior of the ARB can be well simulated by proposed formulations.

References

Asher, J. W., Hoskere, S. N., Ewing, R. D., Van Volkinburg, D. R., Mayes, R. L. and Button, M., 1995, “Seismic Performance of the Base Isolated USC University Hospital in the 1994 Northridge Earthquake.” Proceedings of the 1995 Joint ASME/JSME Pressure Vessels and Piping Conference, HI, USA, Vol. 319, 147-154.

Dowrick D. J., Babor, J., Cousins, W. J. and Skinner, R. I., 1992, “Seismic Isolation of a Printing Press in Wellington, New Zealand.” Bulletin of the New Zealand National Society for Earthquake Engineering, Vol. 25, No. 3, 161-166.

Hamid AHMADI., 2003, "High Damping Natural Rubber Seismic Isolators Historical Development and Performance, " SILER International Workshop 2013, Rome, Italy

Kalpakidis, I. V. and Constantinou, M. C., 2008, “Effects of heating and load history on the behavior of lead –rubber bearings.” Technical Rep. No. MCEER-08-0027, Multidisciplinary Center for Earthquake Engineering Research, Buffalo, N. Y., USA.

Kalpakidis, I. V. and Constantinou, M. C., 2009a, “Effects of heating on the behavior of lead–rubber bearings. I: theory.” Journal of Structural Engineering, ASCE, 135(12):1440-1449 .

Kalpakidis, I. V. and Constantinou, M. C., 2009b, “Effects of heating on the

behavior of lead –rubber bearings. II:verification of theory." Journal of Structural Engineering, ASCE, 135(12):1450-1461.

Kalpakidis, I. V. and Constantinou, M. C., 2010, "Principles of scaling and similarity for testing of lead–rubber bearings. " Earthquake Engineering And Structural Dynamics, Vol. 39, pp.1551-1568.

Skinner, R. I., Tyler, R. G., Heine, A.J. and Robinson, W. H., 1979, "Hysteretic Dampers for the Protection of Structures from Earthquakes." Journal of the New England Water Pollution Control Association Proc. of the South Pac. Reg. Conf. on Earthquake Eng., Wellington, NZ, pp. 643-664.

Mostaghel, N. and Khodaverdian, M., 1987, "Dynamics of resilent -friction base isolation (R-FBI)", Earthquake Engineering and Structural Dynamics, Vol. 15, pp.379-390.

Turkington, D. H., Cooke, N., Moss, P.J. and Carr, A.J., 1989, "Development of a Design Procedure for Bridges on Lead-Rubber bearings." Engineering Structures, Vol. 11, No. 1, 2-8.

M. BOTIŞ. and C. HARBIC., 2012, "A brief history upon seismic isolating systems", Series I: Engineering Sciences, Vol. 5(54), No. 1 .

Naeim, Farzad. and Kelly, J. M., 1999, "Design of Seismic Isolated Structures", John Wiley & Sons, Inc.

Pavot, B. and Polus, E., 1979, "Aseismic Bearing Pads", Tribology International, Vol. 12, No. 3, pp.107-111.

Schektman, N., 1987, "Extending Emergency Procedures: The French Approach", Nuclear Engineering International, Vol. 32, No.398, pp. 61-63

Takahashi, Yoshikazu (2012) "Damage of rubber bearings and dampers of bridges in 2011 great East Japan earthquake." Proceedings of the International Symposium on Engineering Lessons Learned from the 2011 Great East Japan Earthquake, March 1-4, 2012, Tokyo, Japan.

Tsai, C. S., 2015 , " Seismic Isolation Devices: History and Recent Developments." In the 2015 ASME Pressure Vessels and Piping Conference, Seismic Engineering, (ed.) by C. S. Tsai, Cleveland, American Society of Mechanical Engineers, Boston, U. S. A.

Tsai, C. S., 1995, "Seismic Behavior of Buildings with FPS Isolators", Second Congress on Computing in Civil Engineering, 1995, pp.1203-1211.

Tsai, C. S., 1997, "Finite Element Formulations for Friction Pendulum Seismic Isolation Bearings", International Journal for Numerical Methodsin Engineering, Vol. 40(1), pp. 29-49.

Tsai, C. S., Chiang, Tsu-Cheng and Chen, Bo-Jen., 2003, "Component and Shaking Table Tests for Full Scale Multiple Friction Pendulum System", Earthquake Engineering and Structural Dynamics, Vol. 35, No. 13, pp. 1653-1675.

Tsai, C. S., Chiang, Tsu-Cheng and Su, Hui-Chen, 2018, "Innovative Rubber Bearings with Adaptive Characteristics and Extremely High Damping", Proceedings of the 11th National Conference in Earthquake Engineering, Earthquake Engineering Research Institute, Los Angeles, CA. 2018.

Tsai, C. S. (1994) "Temperature effect of viscoelastic dampers during earthquakes, " Journal of Structural Engineering, ASCE, Vol. 120, No. 2, 394-409.

Tsai, C. S. and Lee, H. H. (1993) "Applications of viscoelastic dampers to high-rise buildings, " Journal of Structural Engineering, ASCE, 119(4), 1222-1233.

Tsopelas, P., Constantinou, M. C., Kim, Y. S. and Okamoto, S., 1996, "Experimental Study of FPS System in Bridge Seismic Isolation", Earthquake Engineering and Structural Dynamics, Vol. 25, pp. 65-78.